
BlurNet: Defense by Filtering the Feature Maps

Ravi S. Raju

Department of Electrical Engineering
University of Wisconsin-Madison
Madison, WI 53706
rraju2@wisc.edu

Mikko Lipasti

Department of Electrical Engineering
University of Wisconsin-Madison
Madison, WI 53706
mikko@engr.wisc.edu

Abstract

Recently, the field of adversarial machine learning has been garnering attention by showing that state-of-the-art deep neural networks are vulnerable to adversarial examples, stemming from small perturbations being added to the input image. Adversarial examples are generated by a malicious adversary by obtaining access to the model parameters, such as gradient information, to alter the input or by attacking a substitute model and transferring those malicious examples over to attack the victim model. Specifically, one of these attack algorithms, Robust Physical Perturbations (RP_2), generates adversarial images of stop signs with black and white stickers to achieve high targeted misclassification rates against standard-architecture traffic sign classifiers. In this paper, we propose BlurNet, a defense against the RP_2 attack. First, we motivate the defense with a frequency analysis of the first layer feature maps of the network on the LISA dataset by demonstrating high frequency noise is introduced into the input image by the RP_2 algorithm. To alleviate the high frequency, we introduce a depthwise convolution layer of standard blur kernels after the first layer. Finally, we present a regularization scheme to incorporate this low-pass filtering behavior into the training regime of the network.

1 Introduction

Machine learning has been ubiquitous in various fields like computer vision and speech recognition. [12, 10] However, despite these advancements, neural network classifiers have been found to be susceptible to so called adversarial images [23]. These images are created by altering some pixels in the input space so that a human cannot distinguish it from a natural image but a deep neural network will misclassify the input [9]. This obviously has severe implications considering the rise of self-driving cars and computer vision systems being installed in industrial applications.

Many different types of attacks exist in the deep learning literature. Some of the most popular white-box attacks like the Fast Gradient Sign Method (FGSM) attack and Projected Gradient Descent Attack (PGD) use the gradients of the network to perturb the input [9, 16]. Other attacks such as the Carlini Wagner (CW) attack formulate an optimization problem to minimize the distance \mathcal{D} between an input x and a perturbed input $x + \delta$ such that $x + \delta$ must lie within a specified box constraint with \mathcal{D} being the L_∞, L_2, L_1 distance metric [3]. Yet another class of attacks are those that physically alter the object to be classified with stickers and graffiti which causes the classifier to incur a misclassification [13, 8].

In this paper, we are interested in exploring a defense to the attack proposed in Robust Physical-World Attacks[8]. In that work, the authors designed a general attack algorithm, Robust Physical Perturbations (RP_2) to generate visual adversarial perturbations which are supposed to mimic real-world obstacles to object classification. They sample physical stop signs from varying distances

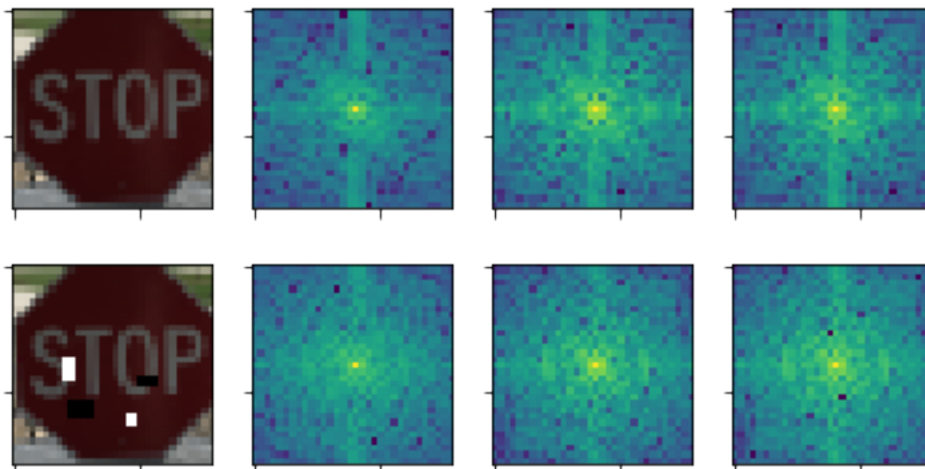


Figure 1: The frequency Spectrum of an unperturbed and perturbed stop sign with a sticker attack. The spectrum has been log-shifted and normalized. Frequencies close to the center correspond to lower frequencies and those that are near the edges correspond to higher ones. Observing the spectrum of the stop sign does not give a clear indication where the perturbations from the stickers lie. Yellow corresponds to regions with most information content.

and angles and use a mask to projected a computed perturbation onto these images. On a standard classifier for road classification, their attack is 100% successful in misclassifying stop signs.

Many defenses use spatial smoothing[14, 25, 15] as means to stamp out the perturbation caused by adversarial attacks. Unfortunately this approach is not always effective if the perturbation is in the form of a peice of tape on a stop sign. To verify this, we plot the Fast Fourier Transorm (FFT) spectrum of a vanilla and perturbed stop sign in Figure 1. Qualitatively, there does not seem to be any significant difference between the two spectrums making filtering the input a questionable defense. Instead, we introduce the simple solution of adding a lowpass filter to perform depthwise convolution after the first layer in the network. The main idea is to curb the spikes in the feature map caused by the perturbations by convolving them with a standard blur kernel. This will attenuate the some of the signal at the output layer but in turn will squash the spikes.

We begin by giving an overview of the RP_2 algorithm and some background on machine learning security. In section 3, we discuss details on adding a filtering layer to dampen high frequency perturbations and perform a blackbox evaluation of RP_2 compared with input filtering. In section 4, we propose a regularization scheme for the network to learn the optimal parameters to incorporate the low-pass filtering behavior using the L_∞ norm and total variation minimization [21]. We then perform a white-box evaluation with RP_2 and find that our algorithm is able to reduce the attack success rate from 90% to 17.5% compared to the baseline classifier.

2 Background

2.1 Problem definition

Consider a neural network to be a function $F(x) = y$, such that $F : \mathbb{R}^m \rightarrow \mathbb{R}^n$, where x is the input image and $m = h * w * c$ such that h, w, c are the image height, image width, and channel number and n is a class probability vector of length of number of classes denoting the class of the image. The goal of an attack algorithm is to generate an image, x_{adv} , so the classifier output mislabels the input image in this manner, $F(x_{adv}) \neq y$. The attack success rate is defined as the number of predictions altered by an attack, that is, $\frac{1}{N} \sum_{n=1}^N \mathbb{1}[F(x_n) \neq F(x_{nadv})]$. Another metric to characterize the

attacker’s success is the dissimilarity distance between natural and adversarial images,

$$\frac{1}{N} \sum_{n=1}^N \frac{\|x - x_{adv}\|_p}{\|x_{adv}\|_p}. \quad (1)$$

where p can take different values depending on the norm chosen; we restrict ourselves to the L_2 case. An adversarial attack is considered strong if the attack success rate is high while having a low dissimilarity distance.

2.2 Attack and Threat Model

We provide a description of the threat model that was considered when developing our defense.

2.2.1 Robust Physical Perturbations Attack

This algorithm is restricted to the domain of road sign classification, focused on finding effective physical perturbations that are agnostic to unconstrained environmental conditions such as distance and the viewing angle of the sign. This is called the Robust Physical Perturbation Attack, known as RP_2 . RP_2 is formulated as a single-image optimization problem which seeks to find the optimal perturbation δ to add an image x , such that the perturbed input $x' = x + \delta$ causes the target classifier, $f_\theta(\cdot)$ to incur a misclassification:

$$\min H(x + \delta, x), \text{ s.t. } f_\theta(x + \delta) = y^*$$

where H is a chosen distance function and y^* is the target class.

To solve the above constrained optimization problem, it must be reformulated as a Lagrangian-relaxed form [3]. The images that are fed into the classifier are mixed in with those from the physical world with those that are synthetically transformed. This is done because approximating the variable physical conditions is difficult with digital synthetic transformations on those images. The synthetic transformations include changing the brightness, cropping the image, and adding other spatial transformations to the input. Eykholt *et al.* model the distribution X^V as the distribution of both the physical and digital images.

Furthermore, this threat model differs from all the others [9, 3, 13] in that the noise introduced must be concentrated on a specific region of image. In the context of road sign classification, an attacker cannot alter the background of the scene so is therefore constrained to the sign. To mimic this effect, a binary mask, M_x , is multiplied with the perturbation, δ , to concentrate the perturbation onto the sign. Since the perturbation is printed in the real world, we need to account for fabrication error, which ensures that the perturbation produced is a valid color in the physical world. This is quantified by the non-printability score (NPS), defined by Sharif *et al.* [22] given by:

$$NPS = \sum_{\hat{p} \in R(\delta)} \prod_{p' \in P} |\hat{p} - p'|,$$

where P is a set of printable colors and $R(\delta)$ is the set of RGB triples used in the perturbation.

The final formulation of the optimization of the perturbation is presented as follows:

$$\operatorname{argmin}_{\delta} \lambda \|M_x \cdot \delta\|_p + NPS + \mathbb{E}_{x_i \sim X^V} J(f_\theta(x_i + T_i(M_x \cdot \delta)), y^*). \quad (2)$$

Here T_i is an alignment function for the masked perturbation that is used to account for if the image, x_i , was transformed so it can be placed optimally. For the distance metric in $\|\cdot\|$, both the L_1 and L_2 norms can be considered. In their experiments, Eykholt *et al.* found that L_1 regularization can find a sparse perturbation vector, attacking the vulnerable regions of the sign. They then recompute the perturbations with another mask placed over these regions with L_2 regularization.

More details on the algorithm can be obtained from [8].

2.2.2 Transferability

Another aspect of these adversarial attack algorithms is the *transferability property*. The idea behind transferability is that adversarial examples that are generated from a model where all the parameters

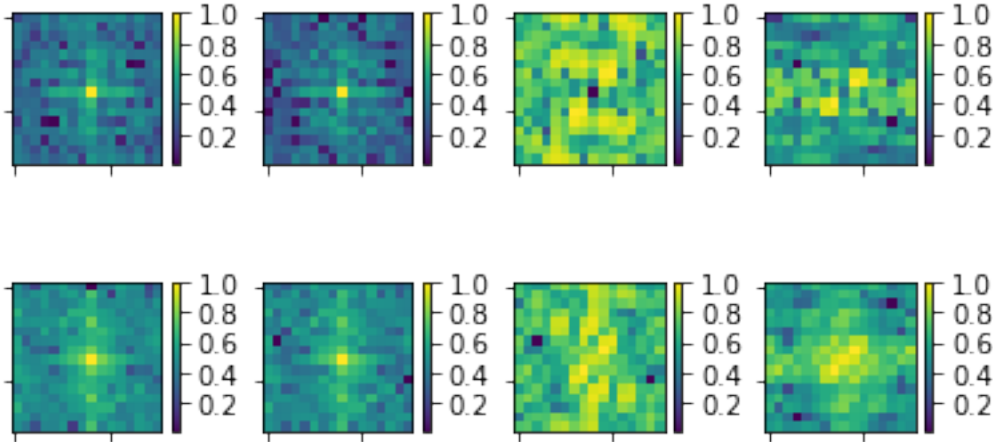


Figure 2: The FFT Spectrum of a subsampling of feature maps from the first layer of the network. Each row corresponds to one unique feature map. The first column is the spectrum of feature maps of an unperturbed stop sign. The second column corresponds to the spectrum of feature maps of a stop sign with the sticker attached. The third column is a difference between the unperturbed and perturbed spectrum. Finally, the fourth column is a blurred version of the difference spectrum. Values were normalized.

are known, can be transferred over to another model that is not known to the attacker. It has been shown these transferability attacks can be performed between different classes of classifiers such as deep neural networks(DNNs), SVMs, nearest neighbors, etc. [18] The motivation for black box attack models arises from this property wherein the adversary is aware of the defense being deployed but does not have access to any of the network parameters or the exact training data [4]. This is the most difficult threat setting for the adversary to operate under as opposed to a white-box setting, in which all the information about the model parameters are known.

2.2.3 Dataset and Model

We adopt the setup from [8] by examining the LISA dataset [1] and a standard 4 layer DNN classifier in the Cleverhans framework [17]. LISA is a standard U.S traffic sign dataset containing 47 various signs, but since there exists a large class imbalance, we only consider the top 18 classes, just as [8]. The network architecture is comprised of 3 convolution layers and a fully-connected layer. We train all the classifiers for 2000 epochs with the ADAM optimizer with $\beta_1 = 0.9$, $\beta_2 = 0.999$, and $\epsilon = 10^{-8}$.

We evaluate our defense based on a sample set of 40 stop sign images provided by [8] from their github repo. When we attempted to recreate the mask to place on the stop sign, we realized that the mask was manually generated after the L_1 optimization of the perturbation. As a result, we directly used the mask provided by the authors for our experiments. We leave the generation of the mask for the evaluation as future work.

3 Motivation

We begin by analyzing the effects of adding a sticker via the RP_2 algorithm from observing the feature maps of the classifier. Understanding differences in activations in both natural and adversarial examples can inform the design of an appropriate defense strategy. When we visualize the feature maps, we can observe an unwanted spike from the activation maps from the first layer in the spatial location where the mask is inserted over the sign. These spikes are large enough that as the activations propagate through the network they cause the classifier to misclassify the input [26, 9]. Based on the assumptions of the threat model, the perturbation is constrained to be on the stop sign, which suggests that the neighboring values around the region of the perturbation are dissimilar in the activation map. In general, we would normally expect smooth transitions in the activation map of images; that is,

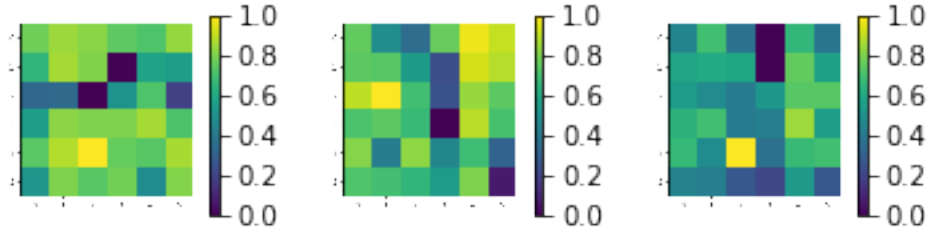


Figure 3: The FFT Spectrum of a subsampling of feature maps from the second layer of the network. These feature maps were obtained from a normal stop sign. The high values indicated at the edges of the spectrum suggests that higher frequency information is relevant to maintain decent classification.

neighbor activations within some spatial window should have approximately similar values. As a motivating example, we applied a standard 5x5 low-pass blur kernel over each of the feature maps. As a result of applying the filter the impact of the spike was substantially smaller.

This initial analysis motivates us to propose a simple solution by applying a set of low-pass filters to the output of first layer of the network. For isolated spikes that are caused by adversarial perturbations, low-pass filters are a natural fit to smooth out unexpected spatial transitions in the activation maps. We focus exclusively on the feature maps after the first layer since spatial locality of the perturbation is still preserved. We insert these filters by performing a depthwise convolution on the feature maps to ensure that the filters are applied independently to each channel [5].

To evaluate the efficacy of inserting the depthwise convolution layer, we transform the feature maps into the frequency domain by computing the Fast Fourier Transform (FFT) of the natural image, adversarial image, and their respective blurred images, as shown in Figure 2. The spectrum is on a log-scale and shifted so points close to the center correspond to lower frequencies and points near the edges to higher frequencies. Based on Figure 2, most of the high frequency artifacts introduced from the perturbations were removed. We do observe some low-frequency components that were induced by the attack, but the influence from these, compared to the high frequency spikes, is much lower.

3.1 Inserting filters in higher layers

We choose only to look at the feature maps after the output of the first layer. We explored adding filters into higher layers of the neural network and we find that these reduce classification accuracy. We hypothesize the reason for this accuracy loss is that the higher layers in the network naturally contain high frequency information. We verify this hypothesis by computing the fast fourier transform of the activations maps of the higher level convolutional layers given in Figure 3. From Figure 3, we can see that the magnitude spectrum shows that the difference between higher and lower frequencies is not pronounced. If a low pass filter is introduced at this level in the network, too much information is lost for the DNN to make a meaningful prediction. In order to maintain classification accuracy, high frequencies in the feature maps should not be squashed. Adding a set of filters to the higher levels of the network is also difficult to justify from a semantic perspective, since the spatial locality of the features is not preserved, as the the receptive field of the neurons in upper layers is wider and even discontinuous due to non-unit convolution strides and/or max-pooling layers.

Table 1: Results from black box evaluation

	Accuracy	Attack Success Rate
Baseline	100%	90%
Input filter 3x3	100%	87.5%
Input filter 5x5	100%	67.5%
3x3 filter on L1 feature maps	100%	65%
5x5 filter on L1 feature maps	87.5%	17.5%

Table 2: Results from white box evaluation

	α	Legitimate Acc.	Average Success Rate	Worst Success Rate	L_2 Distortion
Baseline	0	91%	49.18%	90%	0.207
3x3 conv	10^{-5}	86.3%	30%	55%	0.201
5x5 conv	0.1	86.3%	24.11%	47.5%	0.189
7x7 conv	0.1	87%	11.61%	30%	0.203
TV	10^{-4}	85.6%	7.92%	17.5%	0.224
TV	10^{-5}	82.3%	8.47%	30%	0.199

3.2 Filtering the Input vs. Filtering the feature map

A natural question to ask is what is the motivation for filtering the feature maps over applying the blur kernel over the input image. Our hypothesis is that filtering at the input layer does not remove the perturbation at similar window sizes as filtering the feature maps. To test this hypothesis, we perform a black box transferability attack by generating adversarial examples on the vanilla network and transferring them over to the same model with a blurring filter at the input and one on the feature maps. For our transfer attack, we evaluate the accuracy on a subset of the unperturbed natural stop signs and then measure the attack success rate on the adverserially-perturbed stop signs with $\lambda = 0.002$ and ran for 300 epochs. Our results are shown in Table 1. As seen in Table 1, for lower kernel sizes, while blurring the input does not have much of an impact on the accuracy, it is not effective in alleviating the noise introduced by RP_2 . Compared to blurring the input, adding the blur kernels to the features generated by the first layer seems to effectively reduce the attack success rate at the cost of accuracy. This result motivates an attempt to alter the training regime so it learns the gain parameters in the filter implicitly, rather than setting them to predefined known values, so that robustness can be maintained at a minimal accuracy loss.

4 Learning the Filter Parameters

From the previous section, we see that filtering the feature maps is an effective scheme at discarding the perturbations introduced from RP_2 . However, the side effect of naively inserting a layer of low-pass filters is that the confidence of the prediction is reduced. In certain application domains such as autonomous vehicles, low confidence predictions from the classifier may not be acceptable. For correcting the reduction in the confidence, we seek to incorporate an additional loss term into the training of the classifier. We explore two different options for loss terms: L_∞ norm on the weights of the depthwise layer (added filter layer) and total variance(TV) minimization applied to the feature map (no added layer) [21].

To emulate the effect of adding a layer of low pass filters, the L_∞ norm is an apt choice for the depthwise weights. This will ensure that the weights in the kernel take similar values to each much like a low pass filter. The resulting loss that is minimized, where K is the number of channels in the input, is:

$$\min \alpha \sum_{j=1}^K \|W_{depthwise}[:, :, j]\|_\infty + J(f_\theta(x, y)). \quad (3)$$

Alternatively, we introduce the TV loss term into the optimization algorithm for the classifier, without adding an additional depthwise convolution to the network. Total variation of the image measures the pixel-level deviations for the nearest neighbor and minimizes the absolute difference between those neighbors. For a given image, the TV of an input image x is given as:

$$TV(x) = \sum_{i,j} |x_{i+1,j} - x_{i,j}| + |x_{i,j+1} - x_{i,j}|. \quad (4)$$

In general, the total variation loss is not differentiable so we choose an approximation of the function so that it can be optimized. We omit the depthwise convolution layer from the network and instead let the first layer of the network learn to filter out the high-frequency spikes in its feature map. Defining

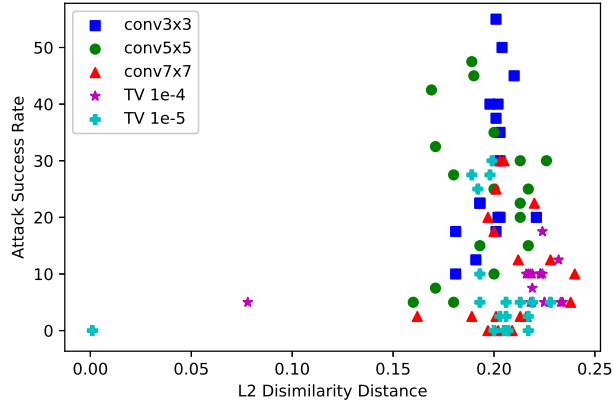


Figure 4: Plot of the L2 Dissimilarity Distance against the Attack Success Rate. Lower and to the right is better.

\mathcal{F} as the set of feature maps after the first layer, the final optimization objective is given as:

$$\min \alpha_{TV} \frac{1}{N \cdot K} \sum_{i=1}^N \sum_{k=1}^K TV(\mathcal{F}[i, :, :, k]) + J(f_{\theta}(x, y)), \quad (5)$$

where N and K are the batch size and the number of output channels, respectively. Intuitively, TV removes effects of details that have high gradients in the image, effectively targeting the perturbations introduced by RP_2 for denoising. TV encourages the neighboring values in the feature maps to be similar so the high spike introduced by RP_2 would be diminished.

We perform a white-box evaluation and sweep the hyperparameters in the attack algorithm, λ and the attack target, y^* . Our results are reported in Table 2. In the white-box setting, the attacker has access to all the model parameters as well as the classification output. The main goal of the evaluation is to detect if the attack algorithm is able to introduce low-frequency perturbations to circumvent the filtering defense. The legitimate accuracy corresponds to the accuracy on the test set. We ran the attack algorithm for 300 epochs. When we sweep the parameters, we find that the attack target is the parameter most sensitive to increasing the success rate of the attack and is relatively invariant to λ . Certain attack targets are more amenable to attacks because there may be steeper gradients of the loss function with respect to those target labels. The legitimate accuracy refers to the accuracy on the test set and the average success rate is the attack success rate averaged across all 17 classes. (We omit the correct class) We also report the best case scenario for the attacker and the L_2 dissimilarity distance.

We find that the TV minimization loss term has superior performance compared to all the other methods, bringing the attack success rate down to 17.5% at a L_2 dissimilarity distance of 0.224. TV is effectively encouraging the first convolutional weight to not only act as a feature extractor but also to stifle high variations coming from the input. For the depthwise convolution layer with the L_{∞} norm regularizer, as the width of the filter increases, the network is able to attenuate the attack success rate because a large window from the surrounding neighbors will be able to smooth out the perturbation. However, the TV loss is better than applying the L_{∞} as it is directly able to influence the weights to behave like a low-pass filter rather than indirectly through the L_{∞} norm. In Figure 4, we plot the L_2 dissimilarity distance against the attack success rate to show the variation of each defense methods across the target labels. We find that TV loss terms have less variation than the other depthwise convolution layers. This supports the previous assertion that the TV term enables the first layer weights to adapt to low-pass behavior.

5 Related Work

Many kinds of defenses have been proposed in the machine learning security literature. There seems to have been two kinds of approaches to developing defenses: robust classification and detection.

Robust classification refers to the classifier being able to correctly classify the input despite the perturbation whereas detection refers to a scheme of identifying if an example has been tampered with and rejecting it from the classifier. Recently, detection methods have seen much more popularity than robust classification (our method belongs to the latter class). However, in certain domains such as autonomous vehicles, it is not always feasible to reject the input from classifier.

Robustness *Adversarial training* is the technique of injecting adversarial examples and the corresponding gold standard labels into the training set [23, 9, 16]. The motivation of this methodology is that the network will learn the adversarial perturbations introduced by the attacker. The problem with adversarial training is that it doubles the training time of the classifier as new examples need to be generated. Moreover, as shown by Papernot et al., adversarial training needs all types of adversarial examples produced by all known attacks, as the training process is non-adaptive [20]. Our method can be paired with any of these types of defenses.

Input transformations Most previous work has applied some type of transform to the input image. In their paper, Guo et. al. use total variance minimization and image quilting to transform the input image. They use random pixel dropout and reconstruct the image with the removed perturbation [11]. Dziugaite et al. examined the effects of JPEG compression on adversarial images generated from the Fast Sign Gradient Method (FGSM) [7, 9]. They report that for perturbations of small magnitude JPEG compression is able to recover some of the loss in classification accuracy, but not always. Xu et al. introduce feature squeezing, a detection method based on reducing the color bit of each pixel in the input and spatially smoothing the input with a median filter [25]. In their paper, Li et al. propose detecting adversarial examples by examining statistics from the convolutional layers and building a cascade classifier. They discover that they are able to recover some of the rejected samples by applying an average filter [14]. Liang et al. looked at using image processing techniques such as scalar quantization and a smoothing spatial filter to dampen the perturbations introduced. The authors introduce a metric, which they define as image entropy, to use different types of filters to smooth the input [15]. We stress that the key difference between these approaches and the proposed methods is that we introduce a change in the model architecture to incorporate it directly into the training process.

Gradient Masking Gradient masking refers to the phenomenon of the gradients being hidden from the adversary by reducing model sensitivity to small changes applied to the input [19]. These can be due to operations that are added to the network that are not differentiable so regular gradient based attacks are insufficient. Another class of gradient masking includes introducing randomization into the network. Stochastic Activation Pruning essentially performs dropout at each layer where nodes are dropped according to some weighted distribution [6]. Xie et al. propose a randomization in which the defense randomly rescales and randomly zero-pads the input to an appropriate shape to feed to the classifier [24]. However, as Athalye et. al have shown in their paper, gradient masking is not an effective defense since the adversary can apply the Backward Pass Differential Approximation attack, in which the attacker approximates derivatives by computing the forward path and backward path with an approximation of the function. Even against randomization, the authors introduce another attack, Expectation over Transformation (EOT), where the optimization algorithm minimizes the expectation of the transformation applied to the input [2].

6 Conclusion

We performed spectral analysis of the feature maps and saw that attacks introduce high-frequency components, which are amenable to low-pass filtering. Our proposal introduced a simple solution of adding low-pass filters after the first layer of the DNN. We compare with this with blurring the input image and show that blurring at the feature level can confer some robustness benefit at the cost of some accuracy by performing a black-box transferability attack with RP_2 . To compensate for the loss in accuracy, we explore two regularization schemes: adding a depthwise convolution and total variation minimization and show that we can recover the loss in accuracy while retaining significant robustness benefit. In the future, we hope to examine more types of attack algorithms and apply them to various datasets with our defense, in addition developing new attacks to circumvent this defense.

References

- [1] Mohan M. Trivedi, Andreas Møgelmo, and Thomas B. Moeslund. Vision based traffic sign detection and analysis for intelligent driver assistance systems: Perspectives and survey. *IEEE Transactions on Intelligent Transportation Systems*, abs/1711.01991, 2012.
- [2] Anish Athalye, Nicholas Carlini, and David A. Wagner. Obfuscated gradients give a false sense of security: Circumventing defenses to adversarial examples. *CoRR*, abs/1802.00420, 2018.
- [3] Nicholas Carlini and David A. Wagner. Towards evaluating the robustness of neural networks. *CoRR*, abs/1608.04644, 2016.
- [4] Nicholas Carlini and David A. Wagner. Adversarial examples are not easily detected: Bypassing ten detection methods. *CoRR*, abs/1705.07263, 2017.
- [5] François Chollet. Xception: Deep learning with depthwise separable convolutions. *CoRR*, abs/1610.02357, 2016.
- [6] Guneet S. Dhillon, Kamyar Azizzadenesheli, Zachary C. Lipton, Jeremy Bernstein, Jean Kossaifi, Aran Khanna, and Anima Anandkumar. Stochastic activation pruning for robust adversarial defense. *CoRR*, abs/1803.01442, 2018.
- [7] Gintare Karolina Dziugaite, Zoubin Ghahramani, and Daniel M. Roy. A study of the effect of JPG compression on adversarial images. *CoRR*, abs/1608.00853, 2016.
- [8] Ivan Evtimov, Kevin Eykholt, Earlene Fernandes, Tadayoshi Kohno, Bo Li, Atul Prakash, Amir Rahmati, and Dawn Song. Robust physical-world attacks on machine learning models. *CoRR*, abs/1707.08945, 2017.
- [9] Ian Goodfellow, Jonathon Shlens, and Christian Szegedy. Explaining and harnessing adversarial examples. In *International Conference on Learning Representations*, 2015.
- [10] Alex Graves, Abdel-rahman Mohamed, and Geoffrey E. Hinton. Speech recognition with deep recurrent neural networks. *CoRR*, abs/1303.5778, 2013.
- [11] Chuan Guo, Mayank Rana, Moustapha Cissé, and Laurens van der Maaten. Countering adversarial images using input transformations. *CoRR*, abs/1711.00117, 2017.
- [12] Alex Krizhevsky, Ilya Sutskever, and Geoffrey E. Hinton. Imagenet classification with deep convolutional neural networks. In *Proceedings of the 25th International Conference on Neural Information Processing Systems - Volume 1, NIPS'12*, pages 1097–1105, USA, 2012. Curran Associates Inc.
- [13] Alexey Kurakin, Ian J. Goodfellow, and Samy Bengio. Adversarial examples in the physical world. *CoRR*, abs/1607.02533, 2016.
- [14] Xin Li and Fuxin Li. Adversarial examples detection in deep networks with convolutional filter statistics. *CoRR*, abs/1612.07767, 2016.
- [15] Bin Liang, Hongcheng Li, Miaoqiang Su, Xirong Li, Wenchang Shi, and Xiaofeng Wang. Detecting adversarial examples in deep networks with adaptive noise reduction. *CoRR*, abs/1705.08378, 2017.
- [16] Aleksander Madry, Aleksandar Makelov, Ludwig Schmidt, Dimitris Tsipras, and Adrian Vladu. Towards deep learning models resistant to adversarial attacks. *CoRR*, abs/1706.06083, 2017.
- [17] Nicolas Papernot, Fartash Faghri, Nicholas Carlini, Ian Goodfellow, Reuben Feinman, Alexey Kurakin, Cihang Xie, Yash Sharma, Tom Brown, Aurko Roy, Alexander Matyasko, Vahid Behzadan, Karen Hambardzumyan, Zhishuai Zhang, Yi-Lin Juang, Zhi Li, Ryan Sheatsley, Abhibhav Garg, Jonathan Uesato, Willi Gierke, Yinpeng Dong, David Berthelot, Paul Hendricks, Jonas Rauber, and Rujun Long. Technical report on the cleverhans v2.1.0 adversarial examples library. *arXiv preprint arXiv:1610.00768*, 2018.

- [18] Nicolas Papernot, Patrick D. McDaniel, and Ian J. Goodfellow. Transferability in machine learning: from phenomena to black-box attacks using adversarial samples. *CoRR*, abs/1605.07277, 2016.
- [19] Nicolas Papernot, Patrick D. McDaniel, Ian J. Goodfellow, Somesh Jha, Z. Berkay Celik, and Ananthram Swami. Practical black-box attacks against deep learning systems using adversarial examples. *CoRR*, abs/1602.02697, 2016.
- [20] Nicolas Papernot, Patrick D. McDaniel, Arunesh Sinha, and Michael P. Wellman. Towards the science of security and privacy in machine learning. *CoRR*, abs/1611.03814, 2016.
- [21] Leonid I. Rudin, Stanley Osher, and Emad Fatemi. Nonlinear total variation based noise removal algorithms. In *Proceedings of the Eleventh Annual International Conference of the Center for Nonlinear Studies on Experimental Mathematics : Computational Issues in Nonlinear Science: Computational Issues in Nonlinear Science*, pages 259–268, New York, NY, USA, 1992. Elsevier North-Holland, Inc.
- [22] Mahmood Sharif, Sruti Bhagavatula, Lujio Bauer, and Michael K Reiter. Accessorize to a crime: Real and stealthy attacks on state-of-the-art face recognition. In *Proceedings of the 2016 ACM SIGSAC Conference on Computer and Communications Security*, pages 1528–1540. ACM, 2016.
- [23] Christian Szegedy, Wojciech Zaremba, Ilya Sutskever, Joan Bruna, Dumitru Erhan, Ian Goodfellow, and Rob Fergus. Intriguing properties of neural networks. In *International Conference on Learning Representations*, 2014.
- [24] Cihang Xie, Jianyu Wang, Zhishuai Zhang, Zhou Ren, and Alan L. Yuille. Mitigating adversarial effects through randomization. *CoRR*, abs/1711.01991, 2017.
- [25] Weilin Xu, David Evans, and Yanjun Qi. Feature squeezing: Detecting adversarial examples in deep neural networks. *arXiv preprint arXiv:1704.01155*, 2017.
- [26] Valentina Zantedeschi, Maria-Irina Nicolae, and Ambrish Rawat. Efficient defenses against adversarial attacks. *CoRR*, abs/1707.06728, 2017.